1-1-2006

Conduction-band electron effective mass in $Zn_{0.87}Mn_{0.13}Se$ measured by terahertz and far-infrared magnetooptic ellipsometry

Tino Hofmann
Institut für Experimentelle Physik II, Fakultät für Physik und Geowissenschaften, Universität Leipzig, 04103 Leipzig, Germany, thofmann4@unl.edu

U. Schade
BESSY GmbH, 12489 Berlin, Germany

K.C. Agarwal
Institut für Angewandte Physik and Center for Functional Nanostructures (CFN), Universität Karlsruhe (TH), 76131 Karlsruhe, Germany

B. Daniel
Institut für Angewandte Physik and Center for Functional Nanostructures (CFN), Universität Karlsruhe (TH), 76131 Karlsruhe, Germany

C. Klingshirn
Institut für Angewandte Physik and Center for Functional Nanostructures (CFN), Universität Karlsruhe (TH), 76131 Karlsruhe, Germany

See next page for additional authors

Conduction-band electron effective mass in $Zn_{0.87}Mn_{0.13}Se$ measured by terahertz and far-infrared magnetooptic ellipsometry

T. Hofmann[a)]
Institut für Experimentelle Physik II, Fakultät für Physik und Geowissenschaften, Universität Leipzig, 04103 Leipzig, Germany

U. Schade
BESSY GmbH, 12489 Berlin, Germany

K. C. Agarwal, B. Daniel, C. Klingshirn, and M. Hetterich
Institut für Angewandte Physik and Center for Functional Nanostructures (CFN), Universität Karlsruhe (TH), 76131 Karlsruhe, Germany

C. M. Herzinger
J.A. Woollam Company, Incorporated, Lincoln, Nebraska 68508

M. Schubert[b)]
Department of Electrical Engineering and Center for Materials Research and Analysis (CMRA), University of Nebraska-Lincoln, 240N WSEC, Lincoln, Nebraska 68588-0511

(Received 31 August 2005; accepted 2 December 2005; published online 24 January 2006)

We determine the electron effective mass parameter $m^*=0.086\pm0.004\ m_0$ of thin-film *n*-type low-chlorine-doped $Zn_{0.87}Mn_{0.13}Se$ with free-charge-carrier concentration $N=4.5\times10^{17}\ cm^{-3}$ and optical mobility $\mu=300\pm20\ cm^2/(V\ s)$ using magneto-optic generalized ellipsometry in the terahertz and far-infrared spectral domain for wave numbers from $\omega=30$–$650\ cm^{-1}$. The room-temperature measurements were carried out with magnetic fields up to 3 T. We employ synchrotron and black-body radiation sources for the terahertz and far-infrared spectral regions, respectively. Comparison with previous experimental results from samples with considerably higher free electron density and theoretical calculations suggest that our value is sufficiently unaffected by band nonparabolicity and provides a good approximation of the Γ-point conduction band mass in $Zn_{0.87}Mn_{0.13}Se$. We further provide optical phonon mode parameters and the high-frequency dielectric constant. © *2006 American Institute of Physics*. [DOI: 10.1063/1.2168258]

$Zn_{1-x}Mn_xSe$ alloys belong to the group of diluted magnetic semiconductors.[1,2] The large Zeeman splitting of the band-edges makes this material suitable either for devising spin filters or using it as a spin aligner in spin-based optoelectronic devices.[3] Crucial for the understanding of the electrical and optical properties is the precise knowledge of intrinsic band structure parameters, such as the Γ-point conduction band curvature and electron mobility, for example.

The conduction band electron effective mass m^* was studied previously as a function of the free-charge-carrier concentration *N* in $Zn_{1-x}Mn_xSe$ alloys for Mn contents of up to $x=0.13$. It was found that the conduction band reveals considerable nonparabolicity effects. For $x=0.13$, m^* at the bottom of the conduction band was predicted applying Kane's model interpolating $m^*(\boldsymbol{k}\neq0)$ toward $m^*(\boldsymbol{k}=0)$ to be smaller by approx. 25% compared with that in the parent compound ZnSe.[4] These experiments were carried out by combined infrared reflection spectroscopy and electrical Hall-effect measurements, and the smallest value of *N* investigated was $1.28\times10^{18}\ cm^{-3}$.[4] Reflection-type intensity infrared measurements on thin film layer structures determine the Drude contribution to the dielectric function upon model calculations, and allow for derivation of parameters m^*, and optical mobility μ, provided *N* is known from an independent measurement, such as a Hall-effect experiment. However, an improved assessment of the conduction-band curvature toward $\boldsymbol{k}=0$, i.e., for small free-charge-carrier densities is desirable not only from a theoretical point of view, but also for future device design. This was left open in our previous work.[4] To the best of our knowledge, infrared optical analysis of low-doped samples for the estimation of the Γ-point effective mass parameter has not been reported yet for $Zn_{1-x}Mn_xSe$.

Here, we present a study of a low-chlorine-doped $Zn_{0.87}Mn_{0.13}Se$ thin film. In this sample, the carrier concentration ($N=4.5\times10^{17}\ cm^{-3}$) is one order of magnitude below the smallest free-electron concentration studied so far.[4] The low doping level in the epilayer was chosen in order to reduce the effect of the conduction-band nonparabolicity on the effective mass parameter.[5,6] We employ our newly developed technique: Magneto-optic generalized ellipsometry (MOGE),[7] which has proven to be a very sensitive tool for the determination of carrier properties in semiconductor thin films and their layer structures.[8,9] We extend here for the first time the spectral range for our technique from the far-infrared to the terahertz region (30 to 650 cm^{-1}) by making use of the infrared and THz synchrotron source IRIS at the electron storage ring BESSY in Berlin, Germany.

Standard (isotropic) ellipsometry determines two independent parameters,[9] which provide access to the complex-valued dielectric function for materials within complex layered systems. Generalized (Mueller matrix) ellipsometry

[a)]Electronic mail: thofmann@rz.uni-leipzig.de
[b)]Electronic mail: mschub@physik.uni-leipzig.de

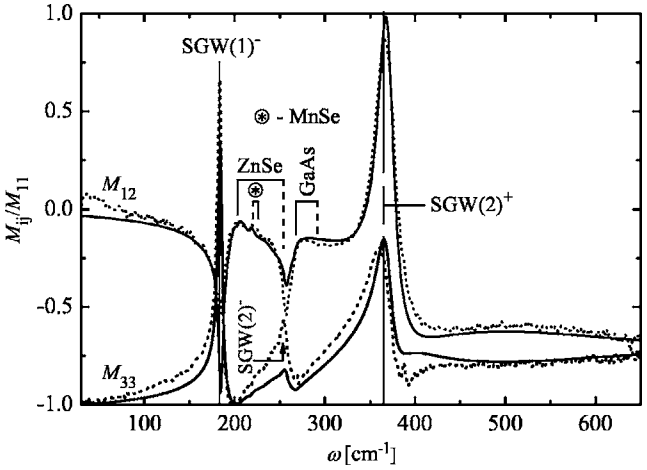

FIG. 1. Field-free ($H=0$) experimental (dotted lines) and best-model calculated (solid lines) spectra of the Mueller matrix elements M_{12} and M_{33}. Note that $M_{21}=M_{12}$, $M_{22}=1$, $M_{13}=M_{23}=M_{31}=M_{32}=0$ were omitted for brevity. Brackets indicate reststrahlen bands of GaAs and $Zn_{0.87}Mn_{0.13}Se$, with solid vertical bars at the TO, and dashed vertical bars at the LO mode frequencies. The asterisk indicates the MnSe-like mode, which splits the ZnSe reststrahlen band.

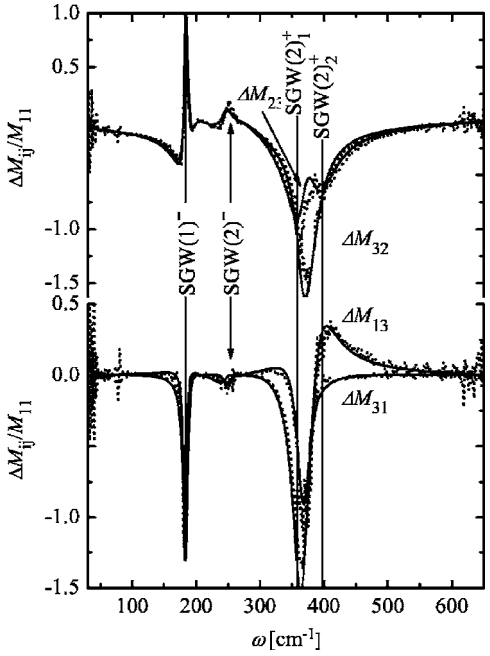

FIG. 2. Experimental (dotted lines) and best-model calculated (solid lines) magnetooptic ellipsometry spectra $\Delta M_{ij}=M_{ij}(\mu_0\boldsymbol{H}=+3\mathrm{T})-M_{ij}(\mu_0\boldsymbol{H}=-3\mathrm{T})$. Note that $\Delta M_{12}=\Delta M_{21}=\Delta M_{22}=\Delta M_{33}=0$ were omitted for brevity.

extends to arbitrarily anisotropic materials, and allows for the determination of the major-axes' dielectric function tensor elements and orientations.[10] The Mueller matrix connects the Stokes vectors describing the general polarization states before ($\boldsymbol{S}_{\mathrm{in}}$) and after ($\boldsymbol{S}_{\mathrm{out}}$) light interaction with the sample: $\boldsymbol{S}_{\mathrm{out}}=\boldsymbol{M}\boldsymbol{S}_{\mathrm{in}}$, where the elements M_{ij}, $(i,j=1\ldots4)$ are usually normalized to M_{11}. MOGE allows the accurate and *simultaneous* determination of parameters m^*, μ, and N by noncontact optical means. In the classical Drude model, the response of free charge carriers subject to an external magnetic field $\mu_0\boldsymbol{H}=\mu_0 H(h_1,h_2,h_3)$ is represented by the following nonreciprocive (chiral) anisotropic tensor:[11]

$$\boldsymbol{\epsilon}^{(\mathrm{FC-MO})}(\omega)=-\omega_p^{*2}\left\{(\omega^2+i\omega\gamma_p)\boldsymbol{I}-i\omega\begin{bmatrix}0 & -h_3 & h_2\\ h_3 & 0 & -h_1\\ -h_2 & h_1 & 0\end{bmatrix}\omega_c\right\}^{-1},$$

where h_1,h_2,h_3 denote the direction cosines of the magnetic field in a Cartesian coordinate system (x,y,z), H is the magnitude of the magnetic field, $\omega_p^{*2}\equiv Ne^2/(\epsilon_0 m^*)$ is the unscreened plasma frequency, $\omega_c\equiv q\mu_0 H/(m^*)$ the cyclotron frequency, and $\gamma_p=q/(\mu m^*)$ is the plasmon broadening parameter.[12] $\boldsymbol{I}$ is the unit tensor, ϵ_0 and μ_0 are the vacuum permittivity and permeability, and $q=-|e|$ is the elementary charge. By use of MOGE, the dielectric polarization response of samples with free-charge carriers subject to external magnetic fields is measured. The latter provides a much improved sensitivity to small carrier responses compared to reflection intensity measurements. In particular, the coupling between longitudinal lattice modes and plasma excitation modes throughout semiconductor layer structures gives rise to dielectric conditions, under which polarized interface modes occur causing distinct resonances in the ellipsometry parameters.[9,13]

A low-chlorine-doped n-type $Zn_{0.87}Mn_{0.13}Se$ epilayer was grown by molecular-beam epitaxy on top of a highly-doped n-type GaAs substrate. The nominal thickness of the $Zn_{0.87}Mn_{0.13}Se$ epilayer was 1500 nm. The Mn composition was determined by Rutherford backscattering and particle induced x-ray emission measurements. A prototype far-infrared ellipsometer setup, operating in the polarizer-sample-rotating-analyzer scheme was used. This instrument determines the Mueller matrix elements M_{ij} except for those in row 4 and column 4, and was equipped with a superconducting magnetocryostat (OXFORD). The sample was placed inside the split-coil arrangement to obtain a 45° angle of incidence where the magnetic field direction pointed parallel to the incident radiation beam (setup "OMO" in Ref. 9). A conventional black-body emitter (silicon carbide globar) and the high-brilliant infrared radiation at the IRIS beamline at BESSY were utilized as independent sources.[14] The ellipsometric measurements were performed in three steps: (*i*) With the magnetic field turned off, (*ii*) set to $\mu_0 H=+3$ T, and (*iii*) $\mu_0 H=-3$ T. Further ellipsometric data were also taken from a reference GaAs substrate for the determination of the free-charge-carrier parameters therein. All data sets were then combined within a model data analysis, where parameterized model functions as described below were varied to match all data sets simultaneously.

A three-phase model (ambient/ZnMnSe layer/GaAs substrate) was employed for model calculations. The dielectric function tensors for both the layer and the substrate were modeled using Drude contributions, as well as Lorentzian broadened harmonic oscillator functions, to account for their polar lattice mode contributions:[8,9,12]

$$\boldsymbol{\epsilon}(\omega)=\epsilon_\infty\prod_{i=1}^{\nu}\frac{\omega^2+i\gamma_{\mathrm{LO},i}\omega-\omega_{\mathrm{LO},i}^2}{\omega^2+i\gamma_{\mathrm{TO},i}\omega-\omega_{\mathrm{TO},i}^2}\boldsymbol{I}+\boldsymbol{\epsilon}^{(\mathrm{FC-MO})}(\omega).$$

Transverse (TO) and longitudinal optical (LO) mode frequency parameters ω_{TO} and ω_{LO} as well as their broadening parameters γ_{TO} and γ_{LO}, respectively, and the high-frequency dielectric constant ϵ_∞ can be derived for each con-

TABLE I. Best-model Drude parameters obtained by ellipsometry data analysis. The uncertainties represent the 90% confidence limits.

	$\omega_c(\mathrm{cm}^{-1})$	$\omega_p(\mathrm{cm}^{-1})$	$\gamma_p(\mathrm{cm}^{-1})$
GaAs substrate	39.5±0.5	1130±13	64±1
$Zn_{0.87}Mn_{0.13}Se$	32.6±0.6	715±23	360±20

TABLE II. Free-charge-carrier parameters obtained from data in Table I. The uncertainties represent the 90% confidence limits.

	$N(10^{17}\ \mathrm{cm}^{-3})$	$m^*(m_0)$	$\mu(\mathrm{cm}^2/(\mathrm{V\ s}))$
GaAs substrate	10.5±0.1	0.071±0.001	20.5±0.1
$Zn_{0.87}Mn_{0.13}Se$	4.9±0.2	0.086±0.002	3.0±0.2

stituent. Parameters for GaAs are given in Ref. 8. For the $Zn_{0.87}Mn_{0.13}Se$ epilayer $\nu=3$, best-model lattice contributions were identified here: $i=1$ (ZnSe-like): $\omega_{TO}=203.4\ \mathrm{cm}^{-1}$, $\omega_{LO}=257.0\ \mathrm{cm}^{-1}$, $\gamma_{TO}=3.6\ \mathrm{cm}^{-1}$, and $\gamma_{LO}=5.5\ \mathrm{cm}^{-1}$; $i=2$ (MnSe-like): $\omega_{TO}=225.3\ \mathrm{cm}^{-1}$, $\omega_{LO}=219.2\ \mathrm{cm}^{-1}$, $\gamma_{TO}=25.7\ \mathrm{cm}^{-1}$, and $\gamma_{LO}=14.6\ \mathrm{cm}^{-1}$; and $i=3$ (additional mode): $\omega_{TO}=217.2\ \mathrm{cm}^{-1}$, $\omega_{LO}=216.7\ \mathrm{cm}^{-1}$, $\gamma_{TO}=6.0\ \mathrm{cm}^{-1}$, and $\gamma_{LO}=10.9\ \mathrm{cm}^{-1}$. As a result, we reveal that ZnMnSe possesses a typical intermediate phonon mode behavior,[15,16] where the MnSe-like modes are located within the ZnSe-like TO and LO mode frequencies. The origin of the additional mode is not clear yet and subject to further work. Further best-model parameters are ZnMnSe thickness $d=1580\pm12$ nm and $\epsilon_\infty=6.2\pm0.1$.

Figure 1 depicts experimental (dotted lines) and best-model calculated (solid lines) ellipsometry data at $H=0$. Spectra acquired by the terahertz ($30\ \mathrm{cm}^{-1}$–$250\ \mathrm{cm}^{-1}$) and far-infrared ($150\ \mathrm{cm}^{-1}$–$650\ \mathrm{cm}^{-1}$) configurations were merged. Within the overlapping wave number regions, data were found highly consistent, and individual spectra are virtually indistinguishable in Fig. 1. All spectra reveal structures caused by the excitation of polarized interface modes [*surface guided waves* (SGW)] and polar lattice modes within the substrate (1) and thin film (2). Dielectric loss situations at specific wave numbers within either substrate (1) or thin film (2) determine conditions for SGW mode occurrence, here at $182\ \mathrm{cm}^{-1}$ [SGW(1)$^-$], $255\ \mathrm{cm}^{-1}$ [SGW(2)$^-$], and $365\ \mathrm{cm}^{-1}$ [SGW(2)$^+$],[9,13] and the strong SGW(2)$^-$ subsumes the weak SWG(1)$^+$ mode not indicated in Fig. 1.

MOGE spectra are shown in Fig. 2, presented as differences between ellipsometry data measured at $\mu_0 H=+3.00\pm0.02$ T and those measured at $\mu_0 H=-3.00\pm0.02$ T. The best-model calculated and the experimental data are in excellent agreement. The magnetic-field-induced optical birefringence is particularly strong near SGW mode resonances. The model calculations for data points in Fig. 2 require only ω_c(GaAs) and ω_c(ZnMnSe) as additional parameters. All other model parameters (lattice mode parameters, $\epsilon_\infty, \omega_p, \gamma_p$) are already defined by matching the spectra in the field-free arrangement in Fig. 1. Table I contains our best-model parameters ω_c, ω_p, and γ_p for both the GaAs substrate and the ZnMnSe epilayer. Table II presents the resulting free-charge-carrier parameters for N, m^*, and μ. The uncertainties of the model parameters correspond to the 90% confidence limits. The obtained tupel $[N,m]$ for GaAs is in good agreement with previously reported values.[5] For $Zn_{0.87}Mn_{0.13}Se$, the tupel $[N,m]=[4.9\pm0.2\times10^{17}\ \mathrm{cm}^{-3}, 0.086\pm0.004\ m_0]$ is found. The band structure parameters required for $\mathbf{k}\cdot\mathbf{p}$ calculations are provided in Ref. 17 which can be used to estimate the effect of nonparabolicity on the effective mass parameter for $N\leqslant5\times10^{17}\ \mathrm{cm}^{-3}$.[5,6] The result is that nonparabolicity deviations from the Γ-point curvature are of smaller magnitude than the error bar in our experiment. Thus, the experimentally obtained value $m^*=0.086\pm0.004\ m_0$ can be taken as a good approximation for the Γ-point effective mass in $Zn_{0.87}Mn_{0.13}Se$. This value also follows the extrapolated trend reported in Ref. 4 from samples with comparable Mn concentration but with much higher electron density N. Furthermore, within the error bar, our value is in good agreement with the theoretically estimated Γ-point conduction-band-edge mass value of $0.093\pm0.009\ m_0$.[4]

In summary, we have applied MOGE employing synchrotron and black-body radiation sources at terahertz and far-infrared spectral ranges for measurement of the free-charge-carrier properties in a low-doped n-type $Zn_{0.87}Mn_{0.13}Se$ thin film, and provide a reliable estimate for the Γ-point conduction-band effective mass in this ternary compound which is in good agreement with previous experimental and theoretical work.

The authors thank D. Spemann, University of Leipzig, for the Rutherford backscattering and particle induced x-ray emission measurements. One of the authors (M.S.) acknowledges support by the Deutsche Forschungsgemeinschaft under Grant No. SCHUH1338/3-1.

[1] O. Goede and W. Heimbrodt, Phys. Status Solidi B **146**, 11 (1988).
[2] J. R. Furdyna, J. Appl. Phys. **64**, R29 (1988).
[3] R. Fiederling, M. Keim, G. Reuscher, W. Ossau, G. Schmidt, A. Waag, and L. W. Molenkamp, Nature (London) **402**, 787 (1999).
[4] K. C. Agarwal, B. Daniel, M. Grün, P. Feinäugle, C. Klingshirn, and M. Hetterich, Appl. Phys. Lett. **86**, 181907 (2005).
[5] A. Raymond, J. Robert, and C. Bernard, J. Phys. C **12**, 2289 (1979).
[6] E. O. Kane, J. Phys. Chem. Solids **1**, 249 (1957).
[7] M. Schubert, T. Hofmann, and C. M. Herzinger, J. Opt. Soc. Am. A **20**, 347 (2003).
[8] T. Hofmann, M. Schubert, C. M. Herzinger, and I. Pietzonka, Appl. Phys. Lett. **82**, 3463 (2003).
[9] M. Schubert, *Infrared Ellipsometry on Semiconductor Layer Structures: Phonons, Plasmons and Polaritons*, Springer Tracts in Modern Physics Vol. 209 (Springer, Berlin, 2004).
[10] M. Schubert, in *Introduction to Complex Mediums for Optics and Electromagnetics*, edited by W. S. Weiglhofer and A. Lakhtakia (SPIE, Bellingham, WA, 2003).
[11] C. Pidgeon, in *Handbook on Semiconductors*, edited by M. Balkanski (North–Holland, Amsterdam, 1980).
[12] P. Yu and M. Cardona, *Fundamentals of Semiconductors* (Springer, New York, 1999).
[13] M. Schubert, T. Hofmann, and J. Šik, Phys. Rev. B **71**, 035324 (2005).
[14] U. Schade, A. Röseler, E. H. Korte, F. Bartl, K. P. Hofmann, T. Noll, and W. B. Peatman, Rev. Sci. Instrum. **73**, 1568 (2002).
[15] L. Genzel, T. Martin, and C. Perry, Phys. Status Solidi B **62**, 83 (1974).
[16] T. R. Yang, C. C. Lu, W. C. Chou, Z. C. Feng, and S. J. Chua, Phys. Rev. B **60**, 16058 (1999).
[17] J. Kvietkova, B. Daniel, M. Hetterich, M. Schubert, D. Spemann, D. Litvinov, and D. Gerthsen, Phys. Rev. B **70**, 045316 (2004).